

Metal Porphyrins for Oxygen Reduction in PEMFC

Yohannes Kiros

Department of Chemical Engineering and Technology, Chemical Reaction Engineering, Royal Institute of Technology (KTH), 100 44 Stockholm, Sweden
E-mail: yohannes@ket.kth.se

Received: 13 December 2006 / *Accepted:* 6 March 2007 / *Published:* 1 April 2007

A short literature review on alternative catalysts for the cathodic oxygen reduction in acid (H_2SO_4) and polymer electrolyte membrane fuel cell (PEMFC) with special emphasis on pyrolyzed macrocycles and precursor materials from metals, organic molecules and N-containing elements has been conducted. Furthermore, various catalytic materials comprising two different concentrations of iron and cobalt tetramethoxyphenyl porphyrins and perovskites were prepared by both the impregnation and precipitation reactions. Screening tests of the individual catalytic materials and their mixtures were carried out in half-cell measurements using the rotating disc electrode (RDE) in 0.5M H_2SO_4 and at room temperature. Cyclic voltammograms were recorded at a scan rate of 10 mV s^{-1} both with and without rotations. The peak potential at 0 rpm was used to study and compare the catalytic activities towards oxygen reduction reaction (ORR). Concentrations of 30wt% Fe and Co/TMPP have shown increased performance characteristics, while those with lower or increased contents, acid-treated and mixed with perovskite have displayed lower activities. Polarization data for the catalyst containing 30wt% Fe/TMPP was also obtained. Acid leaching of the pyrolysis products has resulted in substantial decrease of the metals from the pyrolysis products supported on carbon. TEM, BET-surface area and EDX analyses on the samples have shown high aggregation of the metals with crystalline structure, surface areas depending on the compositions of the catalysts and increased surface concentration of the metals with absence of nitrogen on the moiety.

Keywords: Oxygen reduction; Metal porphyrin; RDE; PEMFC; TEM, BET-surface; EDX

1.0 INTRODUCTION

1.1 Short literature review on alternative catalysts

The challenge of the research and technological development (RTD) of fuel cells, especially that of the PEMFC lies in the catalytic materials for both the anode and cathode. Today's solution of addressing the problem of catalytic reactions for hydrogen oxidation and oxygen reduction is totally

focused on platinum and platinum alloy metals. High power density and efficiency have been achieved, thanks to the high dispersion rates of these nanostructured metals on high surface area carbons. Though the loading of platinum or platinum alloy metals applied as gas diffusion electrodes have been suppressed to a relatively few milligrams per geometric area compared to the efforts done during the 60s and 70s, the question of the replacement of these expensive metals by other active and low cost materials still remains unresolved. Large-scale application (traction or stationary power) and domination in some market segments of fuel cells depend primarily on the issues of demand and supply of the catalysts, duration of operation of these metals and cost of electricity compared to existing power sources. Thus, alternative catalytic materials in either side of the electrodes for PEMFC have a positive impact on future exploitation and application. So far, material research has been mostly based on organic dyestuffs and related materials. An overview of reported studies are presented, while at the same time our findings on similar or different materials are outlined.

Pyrolyzed N_4 -chelates with transition metals supported on high surface area carbons are known to catalytically reduce oxygen in acidic media. Jahnke et al. (1) comparing various organic dyestuffs showed that the N_4 -compounds are active in catalyzing the reduction of oxygen as a result of the interaction between oxygen and the central metal ion based on the model of molecular orbital theory. The first groups of compounds described to be active in electrocatalysis were the phtalocyanines (2), which have a similar structure to the heme groups in the blood pigment, hemoglobin with both compounds surrounded by four nitrogen ligands. Based on comparison of the different types of N_4 -complexes with respect to their activity and stability in acid electrolyte, Alt et al. (3) showed that the porphyrins are to be preferred due to their conjugated π -electron system, a prerequisite for the activation of the oxygen molecule. Thus, the phtalocyanines having similar structure to the base porphyrin, the nitrogen bridges in phtalocyanines do not allow substitution so that electron shifting can take place, thereby affecting the overall activity and stability of the catalyst. In acid electrolytes, the oxygen reduction activity has been correlated to the redox potential of Me^{II}/Me^{III} and to the pyrolysis of the metalloporphyrins with reaction orders of about one for both the heat treated and untreated samples, whereas improved Tafel slopes was obtained by the pyrolyzed products (4).

Although statements about the preservation of the N_4 -metal chelates supported on carbons were forwarded by many other studies, there are however, controversies, conflicting theories and analyses as to how different authors arrive at the conclusions of the structure remaining after heat treatments at high temperatures. Yeager et al. (5) reports that upon contact with an electrolyte solution the metal species may undergo partial or total dissolution. Based on their Mössbauer measurements the only form of Co after heat treatment at 800 °C was found to be cobaltous oxide. In another study Scherson et al. (6) using pyrolysis-mass spectrometry and pyrolysis-gas chromatography-mass spectrometry indicate that the difference in the pyrolysis of the metal-free and metal containing porphyrins can be explained on the basis that the presence of the metal stabilizes the macrocycle ring or that the metal catalyzes pyrolytic processes which result in the binding of the nitrogen in the heat treatment atmosphere. Wiesener (7) based on physical and spectroscopic analytical measurements shows that the elementary composition of nitrogen diminishes with increased annealing temperature and that there are formations of β -cobalt, cobalt carbide or nitride and partly coordination of the central atom with N_4 -ring.

Okabayashi et al.'s (8) description on heat-treated CoTPP (cobalt tetraphenyl porphyrin) by means of DTA-TG (Differential thermal analysis and thermogravimetry) suggests that the molecular weight of the parent molecule decreases by 2.8 times, i.e.; 241 g mol^{-1} and hence a remarkable increase in conductivity and molar magnetic susceptibility is achieved. Analyses by XPS (x-ray photoelectron spectroscopy) of CoTMPP on carbon have shown that oxygen is weakly bonded and that about half of the nitrogen atoms are oxidized during pyrolysis (9). Observations by EELS (Electron Energy Loss Spectroscopy) and TEM have shown that the cobalt metals were slightly oxidized, while nitrogen could not be detected on pyrolyzed CoTPP/carbon at $700 \text{ }^\circ\text{C}$ and some cobalt particles having particle sizes between 10-80 nm were surrounded by carbon substrates (10). A study on pyrolyzed cobalt phthalocyanines (CoPC) by XPS surface concentration analysis has revealed the presence of β -cobalt with increased surface concentration by three-fold already at a heat treatment of $600 \text{ }^\circ\text{C}$, whereas the content of N decreased markedly with increasing pyrolysis temperature reaching its detection limit at $900 \text{ }^\circ\text{C}$ (11). In a similar study (12-15) using XPS and time-of-flight secondary ion mass spectroscopy (ToF-SIMS) on FePC and FeTPP pyrolyzed at $\geq 900 \text{ }^\circ\text{C}$ CoTMPP or at $500\text{-}900 \text{ }^\circ\text{C}$ for CoTAA (cobalt tetraazaannulene), the Fe-N bond was not detected and Fe was mainly observed as a metal surrounded by graphitic coating or particles containing dispersed iron or cobalt (metallic and oxidized) and therefore the catalytic sites were proposed to be ascribed to the inorganic Fe or Co.

The stability of the different types of macrocycles has been an issue regarding oxygen reduction in acid electrolytes for long-term operation. Demetallation of the initially stable cobalt in the form of CoO has been proposed as the reason for the decaying of the catalytic activity of CoTAA (16). Glacial acetic acid treatment of the CoTMPP on carbon, pyrolyzed at $800 \text{ }^\circ\text{C}$, showed that almost half of the cobalt could be extracted, resulting in reduced activity toward O_2 reduction (6). Acid leaching of FeTPP by HCl (13) removed 25% of the bulk iron, albeit superior activity was obtained for the acid washed than the starting material, but the deterioration rate of the catalytic activity was found to be the same. Moreover, CoPC on carbon showed 40% loss of the cobalt after immersion in acid, the consequence of which resulted in a significant decrease of the catalyst performance. Combined acid leaching of the excess Fe in a catalyst containing 10 wt%, H_2SO_4 and Cl_2 (g) treatment at $650 \text{ }^\circ\text{C}$ retained 3.3 wt% Fe and was found to possess increased catalytic activity than its precursor (17).

The dependence on macrocycles with transition metals to prepare active catalysts for the oxygen reduction reaction (ORR) has been recently shown to be superfluous in that the active materials can be directly obtained from heat-treatment of transition metals and N-containing precursors supported on organic molecules or high surface area carbons. In concordant with this new method of preparation, the sources acting as nitrogen-donors may comprise ammonia (NH_3) or acetonitrile (CH_3CN), N-containing pyrroles, a metal salt and carbon materials obtained from pyrolysis of perylenetetracarboxylic dianhydride (PTCDA) or graphite or active carbons or carbon blacks (18-22). ToF-SIMS analysis of the products of Fe on PTCDA or on high surface area carbons, pyrolyzed in a $\text{H}_2/\text{NH}_3/\text{Ar}$ atmosphere and Fe porphyrin showed the presence of FeN_4/C and FeN_2/C catalytic sites with the latter being more pronouncedly active and abundantly represented on the MS (23,24).

Mechanistic studies have also been forwarded by a number of researchers, basically with the rotating ring-disk electrode (RRDE) technique to examine the kinetics of oxygen reduction in acid electrolytes for macrocycle complexes. Yeager (25) reports that CoTSP (cobalt tetrasulfonate

phtalocyanines) promotes oxygen reduction process via $2e^-$ whereas FeTSP has a four-electron pathway. This was explained by the fact that the differences in the redox equilibrium potential of the $\text{Co}^{\text{II}}/\text{Co}^{\text{III}}$ -TSP couple taking place at +0.78V vs. SCE as compared to $\text{Fe}^{\text{II}}/\text{Fe}^{\text{III}}$ -TSP at +0.4V. Therefore, it is suggested that the O_2 binds much easier to the macrocycle complex, oxidizing Fe^{II} to Fe^{III} than the corresponding Co. Unpyrolyzed transition metal macrocycles with cobalt as the central metal atom have shown to be more stable than the corresponding iron complexes, but generate high peroxide yields with n (number of electrons exchanged per oxygen molecule) values of 2-2.5 compared to the Fe-based of $n=3.1-3.4$ (26). Savy et al. (27) proposed the predominance of the $4e^-$ reduction with Tafel slopes of 58-63 mV decade^{-1} for a CoTAA catalyst, promoted by sulfur. Depending on the electrode potential for heat-treated FeTMPP-Cl, n was found to vary between 3.45-4 with almost no influence of the heat-treatment temperature and hence oxygen reduction is to be composed of both direct and series reaction pathways (28). At high potentials, where the current densities are low, the $4e^-$ reduction plays a dominant role in FeTPP-Cl catalyst, while the production of hydrogen peroxide predominates at higher current densities (29). Moreover, Savy et al. (15) found that CoTAA on deoxygenated carbon or with no heat treatment obeyed to a larger extent a $2e^-$ pathway for the oxygen reduction mechanism compared to the heat-treated samples, where the reduction proceeded via the $4e^-$ pathway. Ageing experiments of the catalysts have shown to decrease the n to lower values, confirming the predominance of oxygen reduction via the $2e^-$ pathway for the low temperature or untreated ones while a slight competition of both 2 and $4e^-$ pathways was found to dominate for the high temperature treated macrocycle. Tafel slopes of $-68 \text{ mV decade}^{-1}$ (30) for FeTMPP-Cl heat-treated at 800°C was similar to that of CoTAA (16). However, the Tafel slope at high current densities was found to be higher than the usual and expected value of $-120 \text{ mV decade}^{-1}$. Although an n value of >3.9 and H_2O_2 of $<5 \text{ vol.}\%$ was reported recently (31) for FeTMPP-Cl and Fe on PTCDA, this relatively low concentration of peroxide is believed to decompose the catalytic sites by releasing iron ions into the electrolyte.

Some new perspectives have been taken to develop alternative catalysts by chemical synthesis of other types materials rather than the above mentioned macrocyclic compounds. Perovskites and carbonyl clusters of osmium, ruthenium, molybdenum, and chalcogenides of Mo-Ru-W or Mo-Os-Se and 2,6-bis(imino)-pyridyl complexes have been investigated for their ORR in PEMFC or acid electrolytes (32-38).

2. Our work on alternative catalysts

Based on our experience on alternative catalysts, inter alia materials for ORR on AFC, there is a need to look into the use of these materials in PEFC for the cathode as a replacement for the Pt and Pt-based alloys. Although basically similar activity and mechanism in ORR may take place in both types of FCs in the presence of platinum and platinum alloys, the scope of other catalytic materials and their catalytic properties for oxygen reduction in AFC may differ significantly. The peroxide route in AFC has been found to be a dominating mechanism for a number of catalysts applied on high surface area carbons, which have both the function of a support and a catalyst, leading to the first peroxide generation. In order to assess further application of an AFC catalyst on a PEM cathode, a series of

catalysts with low and high concentrations of Fe and Co with pyrolyzed H₂TMPP and their combination with perovskite (La_{0.1}Ca_{0.9}MnO₃), has to be tested in PEFC. These types of electrocatalysts supported on high surface area carbon black either separately or jointly (39,40) have been shown to possess high catalytic activity and stability in AFC cathodes. To recapitulate our earlier work, catalysts were prepared and screen-tested for their electrochemical oxygen reduction by the rotating disc electrode (RDE), assembled in MEA, analyzed by TEM (transmission electron microscopy) together with EDX (energy dispersive X-ray spectroscopy) as well as surface characterizations by BET-measurements.

2.0 EXPERIMENTAL

1. Preparation of catalysts (CoTMPP and FeTMPP)

Cobalt tetramethoxyphenyl porphyrin and iron tetramethoxyphenyl porphyrins were prepared on high surface area carbons by the impregnation method. Anhydrous cobalt acetate, Co(C₂H₃O₂)₂ 4H₂O, and iron sulphate, Fe(SO₄) 7H₂O, were dissolved in methanol under ultrasonic agitation, whereupon a carbon black (Ketjenblack EC) was added to the solution. Ketjenblack EC-300N has a surface area of 760 m²/g, an average particle size of 30nm and volatile contents of 1%. The mixture was then dried at 60 °C and homogenized in mixer. Meso-tetramethoxyphenyl (H₂TMPP) in varying concentrations was dissolved in concentrated formic acid in ultrasonic bath and the carbon mixture containing the respective metals of Co and Fe were gradually added and soaked in the solution. The slurry was then dried overnight at 80 °C and homogenized again in a mixer. Pyrolysis of the pulverized samples in a holder was carried out at 700 °C in a horizontal quartz tube under a continuous flow of nitrogen for 5 hours. The sample was then withdrawn to a water-cooled zone under a nitrogen atmosphere until the temperature had come down to ambient temperature. The weight compositions of the bulk catalyst mixtures before pyrolysis as prepared and based on pure metallic forms are shown in Table 1.

Table 1. Weight percentage of the bulk transition metal and H₂TMPP on carbon before pyrolysis.

No.	H ₂ TMPP	Carbon	Fe	Co
1	4.61	94.65	-	0.74
2	4.63	94.67	0.70	-
3	27.18	68.45	-	4.37
4	27.30	68.58	4.12	-
5	35.99	58.27	-	5.74
6	36.18	58.37	5.45	-
7	44.67	48.21	-	7.12
8	44.91	48.32	6.77	-

2. La_{0.1}Ca_{0.9}MnO₃ (LCM)

Reagent grade nitrate salts of magnesium, calcium and lanthanum were dissolved in stoichiometric proportions in distilled water under agitation with a magnetic stirrer. These nitrate solutions were then added drop wise to a hot sodium carbonate solution of 1M under constant stirring for 20 minutes. The

precipitate was allowed to settle for an hour so that the supernatant could be decanted. This procedure was repeated several times by washing the precipitate with distilled water to remove the remaining carbonate solution. After this step, the precipitate was filtered off and dried in oven at 120 °C. The dried material was then pulverized in a mixer, subjected to calcination in an oven at 700 °C under a flow of air for 7 hours and withdrawn to remain in a water cooled-zone for half an hour. The LCM prepared in this way was washed to remove small traces of unreacted elements of the starting materials, dried at 120 °C and pulverized in a mixer for further application as electrocatalyst in the test procedures described in section 6.

3. Acid leaching

The pyrolyzed porphyrins with the concentrations indicated in No.3 and 4 (Table 1) were further treated in 1M H₂SO₄, under constant stirring and at a temperature of 80 °C for 6 hours to leach out the excess metals. The catalyst on carbon was filtered, neutralized and washed several times with deionized water. The samples were then dried at 70 °C and homogenized in a mixer to be tested in the RDE.

4. TEM and EDX analyses

Transmission electron microscopy (TEM) and EDX analyses were performed on the CoTMPP and FeTMPP catalysts containing 30 wt.%, viz. No.3 and 4 (Table 1), which showed higher activities for oxygen reduction. Similar analyses were also conducted to the acid-treated materials with the same concentrations in order to assess the morphology and surface elemental compositions.

5. BET-surface area analyses

BET-surface areas, micropore areas, pore volumes and pore diameters of the catalytic materials supported on carbon, consisting of the different concentrations with respective Fe and Co-based pyrolyzed macrocycles as well as perovskite were obtained from nitrogen isotherms (ASAP-2000 Micrometrics). The samples were degassed at 250 °C and nitrogen was adsorbed on the carbon-catalyst and perovskite powders at liquid nitrogen temperature (-196 °C)

6. Rotating disc electrode measurements (RDE)

Electrochemical measurements were carried out in half-cells using the RDE technique. The potentials were measured against Hg/Hg₂SO₄ (MSE) and converted to Hg/Hg₂Cl₂ (SCE) for the purpose of comparing with those reported in the literature data. In order to find out optimal concentrations for the preparation of the ink to be applied on the glassy carbon (GC) a series of trials were made for the adhesion of the electrode materials. Depending on the property of the carbon black, and concentrations of Nafion solution (5% in alcohol) and distilled water mixtures, observations and reiterations were made so that cracks and non-adhesiveness to the substrate were avoided. Finally, 20 mg of catalyst materials and in the case of the CoTMPP/FeTMPP and LCM a 1:1 wt ratio, 200µl Nafion solution and 100µl of distilled H₂O were ultrasonically blended for 30 min. and applied on the GC. 2µl of this ink was then pipetted and evenly spread out on the GC. All measurements were performed at room temperature and 0.5M H₂SO₄ with prior saturation by bubbling oxygen. I-E curves

were recorded for each sample at a scan rate of 10 mV s^{-1} and at 0 rpm and 1000 rpm, respectively. Furthermore, 3 to 4 measurements were done on the same electrode to make an average potential reading of the peak potential (E_p) at 0 rpm and observe the reproducibility under the same operating conditions. More positive potentials or closer values to the thermodynamic reversible potential at ca $+0.985 \text{ V vs. SCE}$ or $+0.585 \text{ V vs. MSE}$, are to be striven after for the ORR (13,24).

7. Membrane Electrode Assembly (MEA) tests.

Galvanostatic and potentiostatic measurements were carried out on a catalyst containing 30 wt.% FeTMPP with iR corrections. The aim of this investigation is to relate the RDE activity data with cell performance characteristics at 60°C and under prolonged time.

3. RESULTS AND DISCUSSION

3.1. Electrochemical assessment

The reference material Ketjenblack EC chemically and thermally treated as the catalytic materials (see section 1 preparation of catalysts), shows a very weak reduction current (ca. $-20 \mu\text{A}$) at -0.15 V vs. MSE and therefore its influence on the overall catalytic activity of the materials examined can be ruled out. Similarly, the individual catalytic activity of the LCM has shown even lower activity than the bare Ketjenblack EC. However, upon repeated cycles in the range of hydrogen and oxygen evolution, major changes of the voltammograms could not be encountered in contrast to the reduction/oxidation current peaks of this perovskite in a microelectrode study in alkaline electrolyte (41). Typical RDE voltammograms for catalysts containing 30 wt% Fe- and CoTMPP are shown in Fig. 1 at 0 rpm, which compared to the other catalysts are superior in activity. At 1000 rpm there was no distinct diffusion plateau for the high performing catalysts. The catalytic activities for ORR of the different single or mixed-type electrodes are also depicted in Table 2.

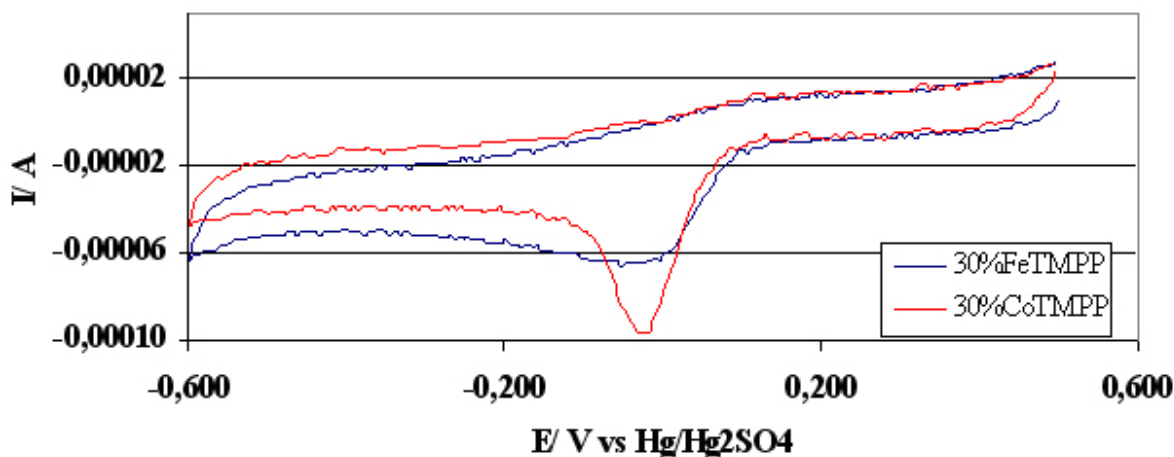


Figure 1. RDE voltammograms of catalysts at a scan rate of 10 mV/s & rpm

The E-I curves scanned between -0.6 to 0.6 V vs. the Hg/Hg₂SO₄ show higher activity toward oxygen reduction with the increasing concentration of the transition metal with the pyrolyzed or charred residue of the porphyrin. Fig. 2 shows how this effect is attributed to the activity for the different sets of catalysts. There is, however a sharp decline of the activity for the Fe-based catalyst compared to the Co-based, where an increase to 40 wt% of Fe is almost on par with a concentration corresponding to the 5% FeTMPP. The increase in CoTMPP over the range of the higher concentrations has not shown substantial decline or upsurge of the activity. However, the catalyst activity decline at higher concentrations generally are slight for the CoTMPP and considerable for the FeTMPP probably due to wettability, mass transfer hindrances as well as surface properties due to higher aggregation of the catalyst particles.

Application of the perovskite on the pyrolyzed catalysts, except for the 5 wt.% CoTMPP, which either with or without LCM showed almost the same activity, had not shown any positive I-E values. The main cause maybe attributed to surface coverage or blockage of the active sites of the pyrolyzed catalysts by the comparably bigger particles with smaller pore volumes, coupled with poor conductivity. Acid-treatment has also shown to change significantly the performance characteristics. Moreover, if these catalysts were to be employed as cathodes in fuel cells, this method would be useful in assessing catalyst dissolution from the bulk material and hence making prior catalyst assessment possible.

Table 2. RDE measurements of the peak potential for ORR for the various catalysts.

Type of Catalyst	Ep mV vs Hg/ Hg ₂ SO ₄	Ep mV vs SCE
5 wt% FeTMPP	-39	+370
30 wt % FeTMPP	+21	+430
30 wt % FeTMPP acid-treated	-24	+386
5 wt % CoTMPP	-44	+365
30 wt % CoTMPP	-1	+408
30 wt % CoTMPP acid-treated	-44	+365
5 wt % FeTMPP+ LCM*	-123	+286
30 wt % FeTMPP+ LCM*	-112	+297
5 wt % CoTMPP+ LCM*	-50	+359
30 wt % CoTMPP+ LCM*	-130	+280
40 wt % FeTMPP	-36	+373
40 wt % CoTMPP	-9	+400
50 wt % FeTMPP	-89	+320
50 wt % CoTMPP	-21	+388

*Admixture of perovskite in 1:1 wt. ratios.

Polarization curves with *iR*-corrections for the gas diffusion electrodes containing 30wt% FeTMPP are presented in Fig. 3. The higher performance among these curves shows catalytic enhancement due to the presence of abundant catalytic sites, non-extracted at the start of the test. Despite the initial lower temperature operation at 40 °C compared to those tested at 60 °C, i.e., 2 and 3, curve 1 shows

high activity at substantial voltages. However, upon consecutive runs of the cell, the current density decreased substantially as related to the potential decline corresponding to the results of the acid-treated RDE samples. The OCV of a commercial Pt-based cell at 60 °C lies at 0.95 V (42), while the cell in this test has 0.75V, mainly ascribable to the activation and dissociative behaviors of oxygen on the catalysts.

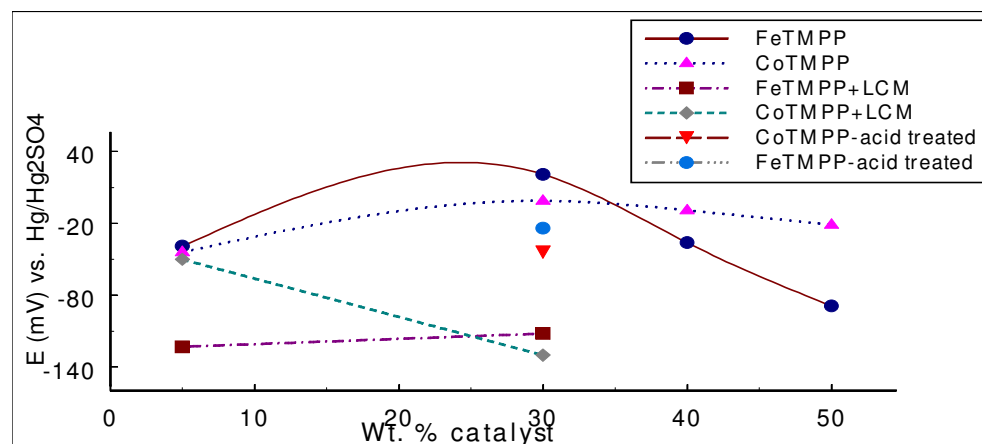


Figure 2. Potential as function of catalyst wt.%, acid-treatment and admixture of perovskite

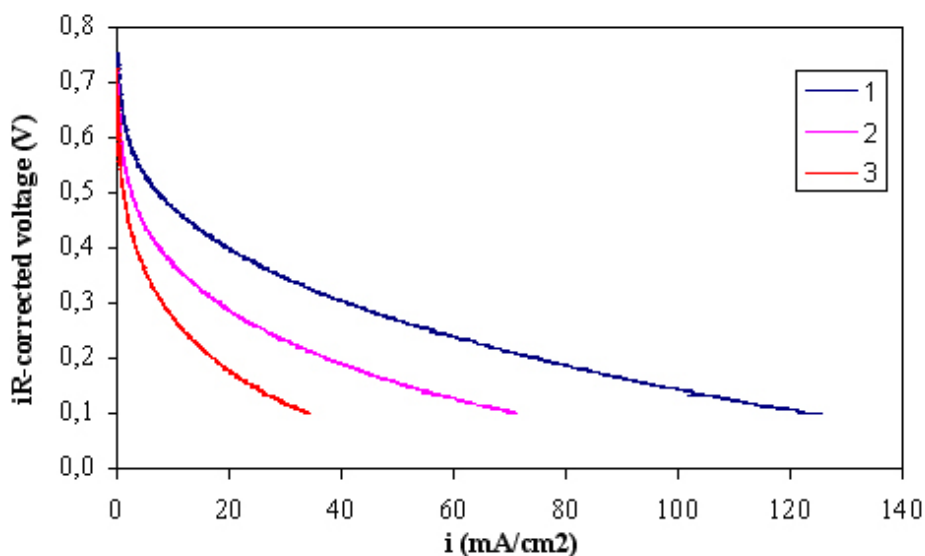


Figure 3. GDE polarization curves for 30 wt% FeTMPP catalyst

An observation of the ohmic losses of the curves due to the contributions from the ionic resistance of the membrane and from the electronic resistance of the electrodes and contacts of the current collectors at a current density of 30 mA/cm² did not result in an increase of R. The voltage drop of 0.226 V between curves 1 and 3 at a current density of 30 mA/cm² implies that the electrode shows instability for long-term operation. However, some further studies of the samples with CoTMPP and those with acid-treatments are presently to be tested in order to have an overall assessment and comparisons of the catalysts for fuel cell operation.

3.2. Surface characterization

Transmission electron microscopy (TEM) analysis of the catalysts with higher concentrations as well as those same materials with the acid-treatment has been carried out. The TEM images of these catalysts are shown in Figures 4-7. The images show that there are abundant and discernible particles from the substrate carbon, having varying particle sizes of 10-400 nm. Higher magnifications of the cobalt-based macrocycles contain bigger particles than 150nm. However, comparisons between FeTMPP and CoTMPP of the TEM images show that the incidence of iron particles has an inclination to have ample agglomerates.

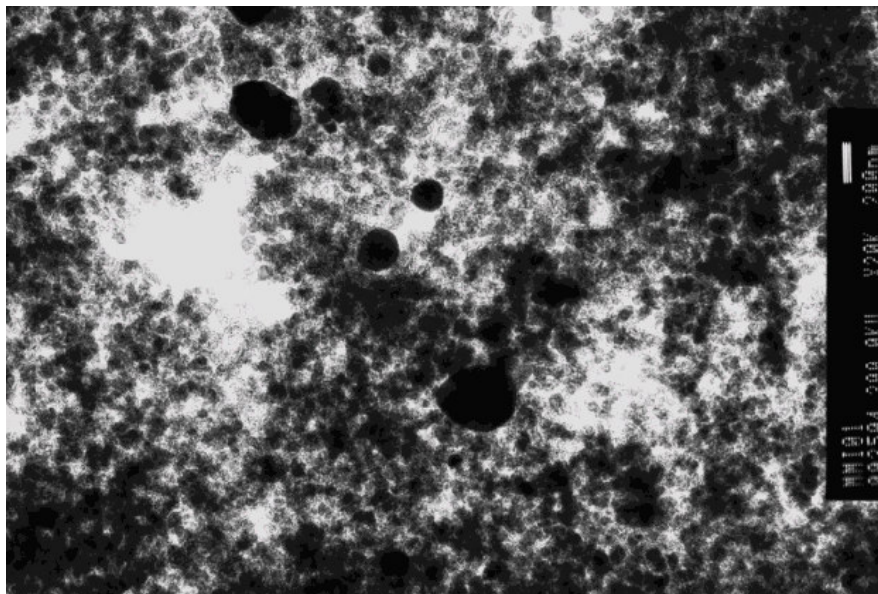


Figure 4. TEM image of 30% FeTMPP applied on carbon after pyrolysis at 700 °C.

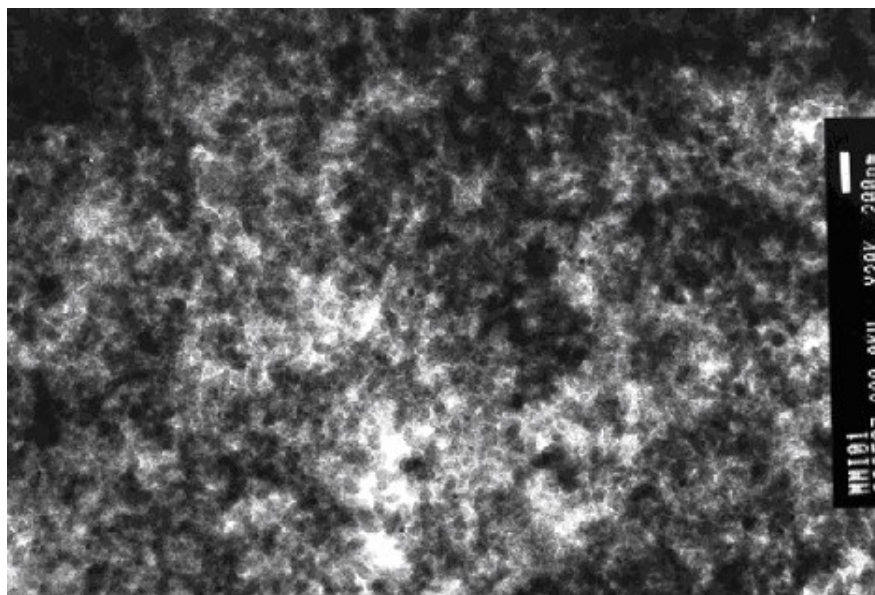


Figure 5. TEM image of 30% CoTMPP applied on carbon after pyrolysis at 700 °C.

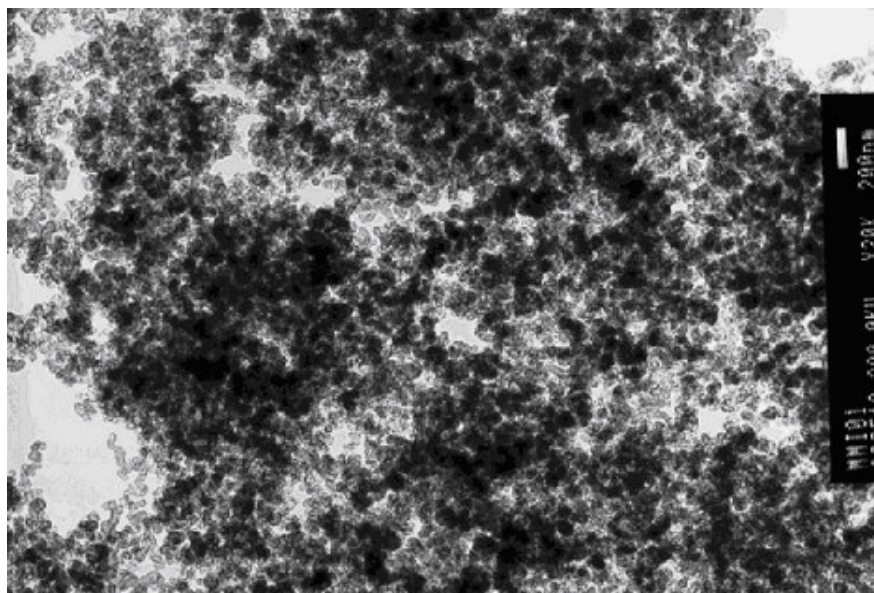


Figure 6. Acid-treated TEM image of 30% FeTMPP catalyst.

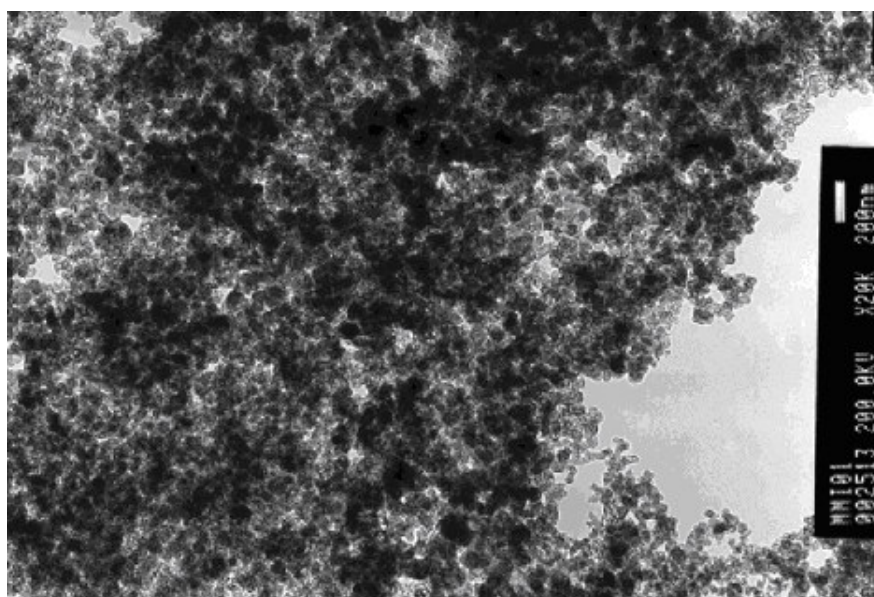


Figure 7. Acid-treated TEM image of 30% CoTMPP catalyst.

The agglomerates, which have coalesced to form clusters during the heat-treatment process or after displacement from the oven, might have been created by migration of small crystallites by virtue of surface energy and diffusion or oxidation by exposure to air. Crystalline structures were observed by directing the probe of the electron beam on single spots of the metal particles. Nevertheless analyses made on the acid-treated samples after pyrolysis, do not show big particles on the carbon substrates, implying that most of the particles were leached out during the treatment. The disposition of the big

clusters has diminished while the remaining particles were surrounded by the protective graphite-like structure.

Quantitative analyses of the elements using EDX have shown the percentage compositions on weight basis, the change of the initial catalysts as compared to Table 1 and the acid-treated samples. Four spectra of each catalyst were recorded from different placements of the specimen and an average of the compositions in weight percent are shown in Table 3. The initial concentrations of both iron and cobalt as shown in Table 1 have increased significantly after pyrolysis, where the heat-treatment produces charred residue of the parent molecules

Table 3. Surface elements of the catalysts analyzed by EDX.

Type	C (wt%)	O (wt%)	Fe (wt%)	Co (wt%)	Total
30%CoTMPP	85.67	3.45		10.88	100
30%FeTMPP	89.29	4.19	6.52		100
30%CoTMPP Acid-treated	88.18	5.76		6.07	100
30%FeTMPP Acid-treated	93.58	4.27	2.16		100

Upon pyrolysis, some of the substituents of the porphyrin molecule are lost giving rise to gaseous products such as CO₂ and CO (8), being evacuated with the flow of nitrogen from the oven. Some of these gases might even react with some surface functional groups of the carbon and in combination with them enrich the total oxygen concentration in the pyrolyzed products compared to the theoretical content of oxygen in the porphyrin of ca. 2.35 wt%. More than doubling of cobalt concentration was exhibited for the pyrolyzed catalysts, implying more likely that Co has a graphitizing effect on the carbon and less bound oxygen per atom cobalt than the iron counterpart. This explains the fact that iron readily interacts with oxygen, resulting in big agglomerates and simultaneous oxide coverage. These oxide coverages of iron if it i) starts in the oven, reacting with the surface oxygen containing groups of carbon or ii) decomposition and reaction of the methoxy substituents of the porphyrin or iii) exposure of the fine particles to air after heat-treatment is not yet clear.

The acid-treated samples show an increase in oxygen concentration for both iron and cobalt, meaning that the iron and cobalt particles might have been oxidized due to handling at the temperature of acid-treatment, exposure to air and subsequent drying at 70 °C. The anhydrous forms of iron and its oxides and cobalt oxides are mostly soluble in sulfuric acid. Therefore, acid leaching shows that more than 2/3 of the iron and ca 50% of the cobalt found in the mixtures of the pyrolysis products are removed. This straightforward method is helpful in finding out the stability of the catalysts at an accelerated rate, before employing them in full-scale lab cell tests. The EDX measurement is appropriate of detecting surface elements from boron (B) down to other elements of the periodic table. Despite the fact that the calculated concentrations of nitrogen in the ingoing porphyrins of FeTMPP and CoTMPP were more than 2wt%, the instrument was not able to detect this element. The instrumental limit of detection for nitrogen lies within $\pm 0.5\text{wt}\%$. Therefore, there is a discrepancy between the descriptions in the literature about the preservation or non-existence of metal-N₄ moiety and the active components found after pyrolysis in our study. However, analysis by XPS is necessary

to assure that the method used for characterization of the pyrolyzed surface elements by EDX is compatible with either of the assertions.

Heat-treatment changes the surface areas, porosities and pore size distributions, chemical as well as electrical properties of not only the catalysts but also of the carbon supports. Carbon blacks without catalysts, which have undergone different thermal and or chemical and physical treatments, have shown to acquire different physicochemical properties (43). BET-surface areas, micropore areas, pore volumes and pore diameter analyses of the catalytic materials supported on carbon and the reference carbon are shown in Table 4. The reference carbon black treated in the same way as the catalysts has high surface area with large micropore areas and pore size diameters of 62 Å. The micropore specific surface area, covering a narrow range dimensions (0.35-2nm), is obtained from the relationship of the volume of adsorbed nitrogen to the thickness t of the ratio of the volume of adsorbed layers, i.e., volume of adsorbed nitrogen to the volume of a monolayer (44,45). More than half of the total BET-surface area of the reference carbon is comprised of micropore areas. However, upon insertion and impregnation of the carbon by the catalysts and the subsequent chemical and heat treatments, the micropore area decreases substantially with increasing concentrations of the catalysts. The same also applies to the total pore volume, where the catalytic materials clog the pores, leading to a total decrease of the available pore volume by more than twice for the higher compared to the lower contents of catalyst. Acid leaching of the catalysts containing 30% of respective Co and FeTMPP shows with the exception for the average pore diameters a decrease of the surface properties. Though larger particles do disappear according to the TEM-analyses, the BET-surface area decrease of 6-12% of these catalysts might be due to the simultaneous removal of the small particle crystallites and/or change of the surface properties of the carbon black due to acid-treatment. Increasing the catalyst content obviously decreases the BET-surface areas of the catalyst on support. But no linear correlations could be extrapolated between concentrations of the catalysts versus BET-surface areas.

Table 4. BET-surface area and porosity measurements of the catalyst materials.

Type of catalyst	BET-surface area (m ² /g)	Micropore area (m ² /g)	Total pore volume (cm ³ /g)	Average pore diameter (nm)
Ketjenblack	752.94	391.89	1.225	6.168
5% FeTMPP	688.58	321.87	1.399	8.211
5% CoTMPP	650.24	311.51	1.038	6.689
30% FeTMPP	268.01	28.42	0.714	10.440
30% CoTMPP	274.26	17.81	0.787	11.303
30% FeTMPP (acid treated)	251.15	13.97	0.697	10.894
30% CoTMPP (acid treated)	242.47	0.11	0.731	11.789
40% FeTMPP	195.39	18.94	0.603	12.543
40% CoTMPP	254.52	18.30	0.635	10.263
50% FeTMPP	136.43	8.76	0.466	13.792
50% CoTMPP	211.62	8.55	0.503	10.116
Perovskite	33.14	-----	0.063	58.711

The perovskite material exhibits very low level of pore volume and BET-surface area having particles with an average pore diameter of 58 nm. In regard to the activity tests of the RDE and in reference to Fig. 2, the most active catalysts have shown to lie in the intermediate BET-surface area ranges.

FeTMPP and CoTMPP and their mixtures with LCM have shown low activity toward ORR. The activity shown with both types of metal porphyrins is therefore a combination of the metallic particles and the charred residues of the macrocycle complex. This activity has been shown to deteriorate in a MEA-test in a short time scale. Further modifications of the catalyst preparations with the help of materials engineering and chemistry, however, may induce to the replacement of the highly scarce and costly Pt or Pt-alloys as cathode materials in PEMFC.

4. CONCLUSION

In conclusion, this study on alternative catalysts for ORR have shown

- an enhancement of catalytic activity for the catalysts containing pyrolysis products of macrocycles with 30 wt% bulk concentrations of Fe or Co
- an admixture of LCM to the macrocycles in the proportions of 1:1 or as bare catalyst has not resulted in any improvement of the performances
- a substantial decrease in stability of a sample containing 30 wt% FeTMPP in a fuel cell test
- acid leaching to remove some active sites in the form of metals or oxide particles may have synergetic effects together with the other active components. 2/3 of the iron and 1/2 of the cobalt have been leached out from the pyrolyzed macrocycle and carbon mixture.
- Analyses of the surface elemental compositions by EDX have not shown any presence of nitrogen after the pyrolysis of the metalloporphyrins
- TEM images show aggregation of clusters as well as the presence of crystalline particles, often surrounded by graphite-like structure comprising both very small and big particles.

ACKNOWLEDGEMENTS

The partial financial support by the Foundation for Strategic Environmental Research (Mistra) is appreciated. RDE measurements by Dr. F. Jaouen, MEA tests by Dr. A. Lundblad and BET-measurements by Mr. M. Pirjamali and their discussions are greatly acknowledged.

References:

1. H. Jahnke, M. Schönborn, G. Zimmermann, *Fortschr. Chem. Fors.*, 61 (1976) 133.
2. R. Jasinski, *Nature*, 201 (1964) 1212.
3. H. Alt, H. Binder, G. Sandstede, *J. Catalysis*, 28 (1973) 8.
4. J. A. R. van Veen, J. F. van Baar, C. J. Kroese, J. G. F. Coolegem, N. de Wit, H. A. Colijn, *Ber. Bunsenges. Phys. Chem.*, 85 (1981) 693.

5. D. A. Scherson, S. L. Gupta, C. Fierro, E. Yeager, M. Kordesch, J. Eldridge, R. Hoffman, *Electrochim. Acta*, 28 (1983) 1205.
6. D. Scherson, A. A. Tanaka, S. L. Gupta, D. Tryk, C. Fierro, R. Holze, E. B. Yeager, R. P. Lattimer, *Electrochim. Acta*, 31 (1986) 1247.
7. K. Wiesener, *Electrochim. Acta*, 31 (1986) 1073.
8. K. Okabayashi, O. Ikeda, H. Tamura, *Chem. Letters*, 1982, 1659.
9. M. Savy, F. Coowar, J. Riga, J. J. Verbist, G. Bronoël, S. Besse, *J. Appl. Electrochem.* 29 (1990) 260.
10. Y. Kiros, S. Schwartz, *J. Power Sources*, 36 (1991) 547.
11. M. Ladouceur, G. Lalande, D. Guay, J. P. Dodelet, L. Dignard-Bailey, M. L. Trudeau, R. Shulz, *J. Electrochem. Soc.*, 140 (1993) 1974.
12. G. Lalande, G. Faubert, R. Côté, D. Guay, J. P. Dodelet, L. T. Weng, P. Bertrand, *J. Power Sources*, 61 (1996) 227.
13. G. Faubert, R. Côté, D. Guay, J. P. Dodelet, G. Dénès, P. Bertrand, *Electrochim. Acta*, 43 (1998) 341.
14. G. Faubert, G. Lalande, R. Côté, D. Guay, J. P. Dodelet, L. T. Weng, P. Bertrand, G. Dénès, *Electrochim. Acta*, 41 (1996) 1689.
15. P. Gouérec, M. Savy, J. Riga, *Electrochim. Acta*, 43 (1998) 743.
16. P. Gouérec, A. Biloul, O. Contamin, G. scarbeck, M. Savy, J. Riga, L. T. Weng, P. Bertrand, *J. Electroanal. Chem.* 42 (1997) 61.
17. G. Faubert, R. Côté, D. Guay, J. P. Dodelet, G. Dénès, C. Poleunis, P. Bertrand, *Electrochim. Acta*, 43 (1998) 1969.
18. G. Lalande, R. Côté, D. Guay, J. P. Dodelet, L. T. Weng, P. Bertrand, *Electrochim. Acta* (1997) 1379.
19. J. Fournier, G. Lalande, R. Côté, D. Guay, J. P. Dodelet, *J. Electrochem. Soc.* 144 (1997) 218.
20. A. L. Bouwkamp-Wijnoltz, W. Visscher, J. A. R. van Veen, S. C. Tang, *Electrochim. Acta* (1999) 379.
21. G. Faubert, R. Côté, J. P. Dodelet, M. Lefèvre, P. Bertrand, *Electrochim. Acta*, 44 (1999) 2589.
22. P. He, M. Lefèvre, G. Faubert, J. P. Dodelet, *J. New Mater. Electrochem. Sys.*, 2 (1999) 243.
23. M. Lefèvre, J. P. Dodelet, P. Bertrand, *J. Phys. Chem. B.*, 106 (2002) 8705.
24. F. Jaouen, S. Marcotte, J. P. Dodelet, G. Lindbergh, *J. Phys. Chem. B.*, 107 (2003) 1376.
25. J. Zagal, P. Bindra, E. Yeager, *J. Electrochem. Soc.*, 127 (1980) 1506.
26. A. S. Lin, J. C. Huang, *J. Electroanal. Chem.*, 541 (2003) 147.
27. O. Contamin, C. D-Chouvy, M. Savy, G. Scarbeck, *Electrochim. Acta*, 45 (1999) 721.
28. S. Lj. Gojković, S. Gupta, R. F. Savinell, *Electrochim. Acta*, 45 (1999) 889.
29. A. L. B-Wijnoltz, W. Visscher, J. A. R. van Veen, *Electrochim. Acta*, 43 (1998) 3141.
30. S. Lj. Gojković, S. Gupta, R. F. Savinell, *J. Electroanal. Chem.*, 462 (1999) 63.
31. M. Lefèvre, J. P. Dodelet, *Electrochim. Acta*, 48 (2003) 2749.
32. J. R. Juado, E. Chinaro, M. T. Colomer, *Solid State Ionics*, 135 (2000) 365.
33. O. S-Feria, S. C-Cigarroa, R. R-Noriega, S. M. F-Valverde, *Electrochem. Comm.*, 1 (1999) 585.
34. F. J. Rodriguez, P. J. Sebastian, O. Solorza, R. Pérez, *Int. J. Hydrogen Energy*, 23 (1998) 1031.
35. M. Bron, P. Bogdanoff, S. Feichter, M. Hilgendorff, J. Radnik, I. Dorbandt, H. Schulenburg, H. Tributsch, *J. Electroanal. Chem.*, 517 (2001) 85.
36. P. J. Sebastian, *Int. J. Hydrogen Energy*, 255.
37. R. H. Castellanos, A. L. Ocampo, J. M-Acosta, P. J. Sebastian, *Int. J. Hydrogen Energy*, 26 (2001) 1301.
38. J. Jiang, A. Kucernak, *Electrochim. Acta*, 47 (2002) 1967.
39. Y. Kiros, C. Myrén, S. Schwartz, A. Samapthrajan, M. Ramanathan, *Int. J. Hydrogen Energy*, 24 (1999) 549.

40. Y. Kiros, S. Schwartz, *J. Power Sources*, 36 (1991) 547.
41. M. Bursell, M. Pirjamali, Y. Kiros, *Electrochim. Acta*, 47 (2002) 1651.
42. Y. W. Rho, O. A. Velev, S. Srinivasan, *J. Electrochem. Soc.*, 141 (1994) 2084.
43. M. Pirjamali, Y. Kiros, *J. Power Sources*, 109 (2002) 446.
44. J. W. Patrick, *Porosity in Carbons*, Edward Arnold, London, 1995, p. 67.
45. K. Kinoshita, *Carbon electrochemical and physicochemical properties*, John Wiley & Sons, 1988, p. 40.